Progress In Electromagnetics Research M, Vol. 25, 173–184, 2012

REALIZATION OF THE PERFECT ELECTROMAGNETIC CONDUCTOR CIRCULAR CYLINDER USING ANISOTROPIC MEDIA

N. Montaseri*, M. Soleimani, and A. Abdolali

Antenna Research Laboratory, School of Electrical Engineering, Iran University of Science and Technology (IUST), Iran

Abstract—In this paper, an analytical solution is investigated for the two-dimensional problem of electromagnetic scattering of a line source from a perfect electromagnetic conductor (PEMC) circular cylinder coated with an anisotropic media. In the anisotropic region, the relative permittivity and permeability tensors, when referred to principal axes (ρ, ϕ, z), are biaxial and diagonal. It is demonstrated that the relations of electromagnetic field vectors in anisotropic medium is equal to a PEMC boundary conditions when the parameters of the anisotropic region are chosen in an appropriate manner. Therefore, this region can act as a PEMC cylinder.

1. INTRODUCTION

The concept of Perfect Electromagnetic Conductor (PEMC) has been defined by linear medium equations so that the relations of field vectors take the forms [1]

$$\vec{H} = -M\vec{E}, \quad \vec{D} = M\vec{B} \tag{1}$$

where M represents a real scalar admittance-type quantity. Also the complex Poynting vector is an imaginary one, and the electromagnetic energy cannot enter the PEMC medium [2, 3]. For two special cases of $M \to \pm\infty$ and $M = 0$, PEMC decreases to more ordinary perfect electric conductor (PEC) and perfect magnetic conductor (PMC), respectively. As a result, the PEMC boundary condition is [4]

$$\hat{n} \times (\vec{H} + M\vec{E}) = 0 \tag{2}$$

where $\hat{n}$ is the unit vector normal to the surface of the PEMC.

Received 20 June 2012, Accepted 30 July 2012, Scheduled 10 August 2012

* Corresponding author: Nasser Montaseri (montaseri@elec.iust.ac.ir).

The analytical solution of line source of scattering from PEC and PEMC circular cylinder coated with isotropic media was investigated in [5, 6], respectively. Furthermore, plane wave scattering by a composite circular cylindrical structure was illustrated using PEC [7] as well as PEMC core [8]. Also, scattering of PEMC structures for practical applications was investigated in [9, 10]. The PEMC was initially introduced as a purely conceptual medium. Afterwards, the realization of PEMC boundary has been studied, and a grounded ferrite slab has practically represented a PEMC boundary condition in Cartesian coordinate [11], but in the cylindrical coordinate it has not been studied yet.

The organization of this paper is as follows. In Section 2, the response of an anisotropic coated PEMC cylinder to the line source radiation is studied, and the total fields are determined in all regions. It was demonstrated that the anisotropic medium can act as PEMC cylinder with $M\eta_0 = \pm 1$. In Section 3, some numerical examples are provided and compared with the published literature [5, 8]. The were found in good agreement. Finally, summary and conclusions are provided in Section 4.

2. THEORY

The cross-section of an infinite PEMC cylinder coated with anisotropic media is shown in Fig. 1. The structure excited by a line source of current I_e with uniform phase and amplitude is along the z-axis at the point of cylindrical coordinate (ρ_0, ϕ_0). The PEMC core has radius $\underline{a}$, and the anisotropic sleeve has thickness $\underline{b-a}$.

In the anisotropic layer, $a \leq \rho \leq b$, the relative permittivity and permeability tensors referred to the cylindrical coordinate are given by

$$\bar{\bar{\varepsilon}} = \begin{bmatrix} \varepsilon_1 & 0 & 0 \\ 0 & \varepsilon_2 & 0 \\ 0 & 0 & \varepsilon_3 \end{bmatrix}_{\rho\phi z} \quad ; \quad \bar{\bar{\mu}} = \begin{bmatrix} \mu_1 & 0 & 0 \\ 0 & \mu_2 & 0 \\ 0 & 0 & \mu_3 \end{bmatrix}_{\rho\phi z} \tag{3}$$

In this region, there are two polarizations completely independent of each other, and the radial eigenfunctions satisfy Bessel functions

Table 1. Anisotropic media.

Polarization	TM_z	TE_z
Bessel function argument	$u = k_0\rho\sqrt{\mu_2\varepsilon_3}$	$v = k_0\rho\sqrt{\varepsilon_2\mu_3}$
Bessel function order	$\nu_e = n\sqrt{\mu_2/\mu_1}$	$\nu_m = n\sqrt{\varepsilon_2/\varepsilon_1}$

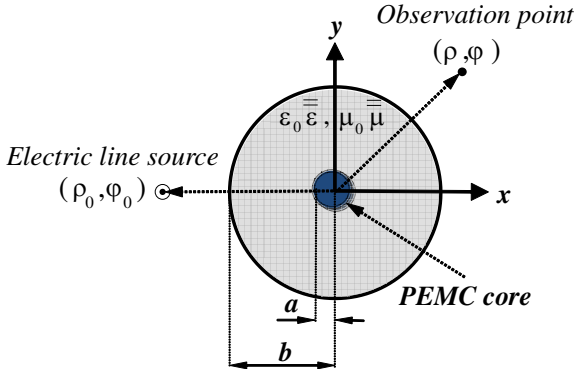

Figure 1. Cross section of geometry.

with complex order and argument [7], which is shown in Table 1. It is obvious that TE_z and TM_z polarizations depend on completely separate sets of constitutive parameters, i.e., μ_1, μ_2 and ε_3 for TM_z and ε_1, ε_2 and μ_3 for TE_z. As an interesting result, one mode can be used with negative parameters and the other with positive ones (but in the isotropic region, it is not possible).

In this paper, the scattering of electric line source (TM_z) placed outside anisotropic region was considered. However, using the duality principle, the problem can be solved for magnetic line source (TE_z). In the expressions for the electromagnetic fields, the time-dependence factor $\exp(j\omega t)$ is suppressed. The solution spaces can be separated into three regions, Region I for $\rho \geq \rho_0$, Region II for $b \leq \rho \leq \rho_0$ and Region III for $a \leq \rho \leq b$. By using the addition theorem for Hankel functions [12], the incident electric field from the line source (I_e) can be expressed as

$$E_z^{inc}(\rho,\phi) = \frac{-k_0^2 I_e}{4\omega\varepsilon_0} \begin{cases} \displaystyle\sum_{n=-\infty}^{+\infty} J_n(k_0\rho_0)\, H_n^{(2)}(k_0\rho)\, e^{jn(\phi-\phi_0)}; & \rho \geq \rho_0 \\ \displaystyle\sum_{n=-\infty}^{+\infty} J_n(k_0\rho)\, H_n^{(2)}(k_0\rho_0)\, e^{jn(\phi-\phi_0)}; & \rho \leq \rho_0 \end{cases} \tag{4}$$

where $J_n(k_0\rho)$ and $H_n^{(2)}(k_0\rho)$ represent Bessel function of the 1st kind and Hankel function of the 2nd kind, respectively. Also, in all the formulations, prime denotes the derivative with respect to the entire argument. Therefore, the total fields in Region I, $\rho \geq \rho_0$, are given by

the following expressions

$$E_z^I = \frac{-k_0^2 I_e}{4\omega\varepsilon_0} \sum_{n=-\infty}^{+\infty} H_n^{(2)}(k_0\rho)\Big[J_n(k_0\rho_0)+a_n H_n^{(2)}(k_0\rho_0)\Big] e^{jn(\phi-\phi_0)} \quad (5)$$

$$H_\phi^I = \frac{-k_0 I_e}{j4} \sum_{n=-\infty}^{+\infty} H'^{(2)}_n(k_0\rho)\Big[J_n(k_0\rho_0)+a_n H_n^{(2)}(k_0\rho_0)\Big] e^{jn(\phi-\phi_0)} \quad (6)$$

$$H_z^I = \frac{-k_0 I_e}{j4} \sum_{n=-\infty}^{+\infty} H_n^{(2)}(k_0\rho)\Big[b_n H_n^{(2)}(k_0\rho_0)\Big] e^{jn(\phi-\phi_0)} \quad (7)$$

$$E_\phi^I = \frac{-k_0^2 I_e}{4\omega\varepsilon_0} \sum_{n=-\infty}^{+\infty} H'^{(2)}_n(k_0\rho)\Big[b_n H_n^{(2)}(k_0\rho_0)\Big] e^{jn(\phi-\phi_0)} \quad (8)$$

where $k_0 = \omega\sqrt{\varepsilon_0\mu_0}$ is the wavenumber in free space. The total fields in the Region II, $b \le \rho \le \rho_0$, could be written as

$$E_z^{II} = \frac{-k_0^2 I_e}{4\omega\varepsilon_0} \sum_{n=-\infty}^{+\infty} H_n^{(2)}(k_0\rho_0)\Big[J_n(k_0\rho) + a_n H_n^{(2)}(k_0\rho)\Big] e^{jn(\phi-\phi_0)} \quad (9)$$

$$H_\phi^{II} = \frac{-k_0 I_e}{j4} \sum_{n=-\infty}^{+\infty} H_n^{(2)}(k_0\rho_0)\Big[J'_n(k_0\rho)+a_n H'^{(2)}_n(k_0\rho)\Big] e^{jn(\phi-\phi_0)} \quad (10)$$

$$H_z^{II} = \frac{-k_0 I_e}{j4} \sum_{n=-\infty}^{+\infty} H_n^{(2)}(k_0\rho_0)\Big[b_n H_n^{(2)}(k_0\rho)\Big] e^{jn(\phi-\phi_0)} \quad (11)$$

$$E_\phi^{II} = \frac{-k_0^2 I_e}{4\omega\varepsilon_0} \sum_{n=-\infty}^{+\infty} H_n^{(2)}(k_0\rho_0)\Big[b_n H'^{(2)}_n(k_0\rho)\Big] e^{jn(\phi-\phi_0)} \quad (12)$$

And the total fields in Region III, $a \le \rho \le b$, is [7]

$$E_z^{III} = \frac{-k_0^2 I_e}{4\omega\varepsilon_0} \sum_{n=-\infty}^{+\infty} H_n^{(2)}(k_0\rho_0)\Big[c_n J_{\nu_e}(u) + d_n H_{\nu_e}^{(2)}(u)\Big] e^{jn(\phi-\phi_0)} \quad (13)$$

$$H_\phi^{III} = \frac{-k_0 I_e}{j4} Y_e \sum_{n=-\infty}^{+\infty} H_n^{(2)}(k_0\rho_0)\Big[c_n J'_{\nu_e}(u)+d_n H'^{(2)}_{\nu_e}(u)\Big] e^{jn(\phi-\phi_0)} \quad (14)$$

$$H_z^{III} = \frac{-k_0 I_e}{j4} Y_e \sum_{n=-\infty}^{+\infty} H_n^{(2)}(k_0\rho_0)\Big[e_n J_{\nu_m}(v)+f_n H_{\nu_m}^{(2)}(v)\Big] e^{jn(\phi-\phi_0)} \quad (15)$$

$$E_\phi^{III} = \frac{-k_0^2 I_e}{4\omega\varepsilon_0} Y_e Z_m \sum_{n=-\infty}^{+\infty} H_n^{(2)}(k_0\rho_0)\Big[e_n J'_{\nu_m}(v)+f_n H'^{(2)}_{\nu_m}(v)\Big] e^{jn(\phi-\phi_0)} \quad (16)$$

where $\nu_e = n\sqrt{\mu_2/\mu_1}$, $\nu_m = n\sqrt{\varepsilon_2/\varepsilon_1}$, $u = k_0\rho\sqrt{\mu_2\varepsilon_3}$, $v = k_0\rho\sqrt{\varepsilon_2\mu_3}$, $Y_e = \sqrt{\varepsilon_3/\mu_2}$, and $Z_m = \sqrt{\mu_3/\varepsilon_2}$. In order to determine the unknown coefficients a_n, b_n, c_n, d_n, e_n, and f_n, the following boundary conditions need to be applied.

(a) at $\rho = a$ and $0 \leq \phi \leq 2\pi$. The PEMC boundary condition can be written as

$$H_z^{III} + ME_z^{III} = 0 \tag{17}$$

$$H_\phi^{III} + ME_\phi^{III} = 0 \tag{18}$$

(b) at $\rho = b$ and $0 \leq \phi \leq 2\pi$. Also, the tangential components of the total electric and magnetic fields should be continuous

$$E_z^{II} = E_z^{III} \tag{19}$$

$$H_\phi^{II} = H_\phi^{III} \tag{20}$$

$$H_z^{II} = H_z^{III} \tag{21}$$

$$E_\phi^{II} = E_\phi^{III} \tag{22}$$

By applying these boundary conditions, the linear matrix equation about the unknown coefficients was obtained (see Appendix A), which could be used to acquire the co- and cross-polarized fields in all regions. Appendix A shows that for $M\eta_0 = \pm 1$, $0 < a \leq b$, and anisotropic lossless media with $\varepsilon_1 = \varepsilon_2 = -\mu_1 = -\mu_2$, $\varepsilon_3 = -\mu_3$ (ε_3 and μ_2 have the same sign), the relations between electric and magnetic fields satisfy the following equations.

$$\vec{H}^{III} + M\vec{E}^{III} = 0 \tag{23}$$

$$\vec{D}^{III} - M\vec{B}^{III} = 0 \tag{24}$$

Equations (23) and (24) demonstrate the realization of PEMC media using anisotropic coating. Using anisotropic layer and small PEMC core with radius $\underline{a}$, the PEMC circular cylinder can be realized with larger radius of $\underline{b}$. This result can be useful in microwave engineering as well as antenna engineering. Potential practical applications, such as a boundary, are, e.g., for field pattern purifiers for aperture antennas (also in circular structures), polarization transformers, and radar scatters. Appendix B shows that when the line source is placed at far distance ($k_0\rho_0 \gg 1$) and the observation points located at Region II ($b \ll \rho < \rho_0$), the problem is converted to the plane wave scattering by PEMC circular cylinder coated with anisotropic media, and the radar cross section (RCS) of the structure can be calculated. On the other hand, this problem is more general than the scattering of incident plane wave.

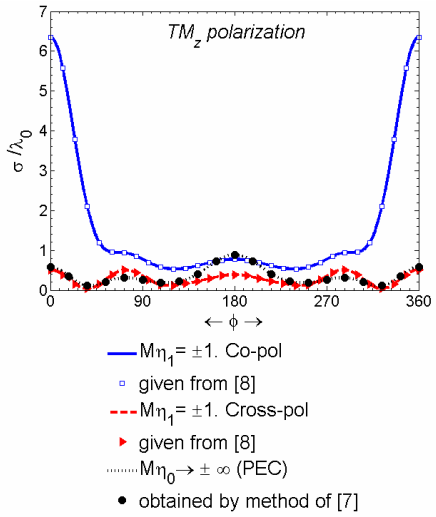

Figure 2. Normalized bistatic scattering cross-section of a coated PEMC cylinder ($a = 5\,\text{cm}$, $b = 10\,\text{cm}$, $f = 1\,\text{GHz}$).

3. SIMULATIONS AND APPLICATIONS

In this section, some numerical results are presented and compared with those in the published literature [5, 8], and the analytical formulations were verified. In all the plots, line source is placed at (ρ_0, $\phi_0 = 180°$), and λ_0 is the wavelength of free space. According to Fig. 2, the line source was placed at far distance from the structure ($k_0\rho_0 \gg 1$, $\rho < \rho_0$) with frequency of 1 GHz. Hence, the bistatic Radar Cross Section (RCS) was considered by a circular PEMC cylinder coated with anisotropic media (see Appendix B). The radii of PEMC core cylinder and coating cylinder were considered 5 and 10 cm, respectively. For $M\eta_1 = \pm 1$ ($\eta_1 = \eta_0\sqrt{\mu_1/\varepsilon_1}$), the anisotropic layer with relative permittivity $\varepsilon_1 = \varepsilon_2 = \varepsilon_3 = 9.8$ and permeability $\mu_1 = \mu_2 = \mu_3 = 1$ was compared with a published paper [8], and good agreement was found between them. Also, for $\varepsilon_1 = 9.8$, $\varepsilon_2 = 16$, $\varepsilon_3 = 7$, $\mu_1 = 1$, $\mu_2 = 19$, and $\mu_3 = 6$. Scattering by a PEC cylinder coated with anisotropic medium is calculated using method of [7] and compared with a coated PEMC cylinder with $M\eta_0 \to \pm\infty$ (where PEMC acts as PEC). This comparison shows an excellent agreement between the co-polarized components of the bi-static cross-sections and validates the presented relations and results. Clearly, the cross-polarized component of the bi-static cross-section of coated PEMC with $M\eta_0 \to \pm\infty$ is equal

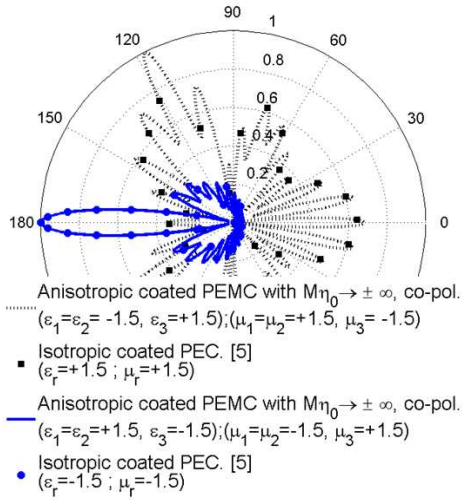

Figure 3. Far-field radiation patterns of electric line source outside a coated PEMC cylinder. ($a = 1.25\lambda_0$, $b = 2.25\lambda_0$, $\rho_0 = 2.3\lambda_0$).

to zero.

In Fig. 3, the far field radiation patterns of the anisotropic coated PEMC cylinder are demonstrated when $a = 1.25\lambda_0$, $b = 2.2\lambda_0$, $\rho_0 = 2.3\lambda_0$. It is obvious that for $M\eta_0 \to \pm\infty$, the behavior of PEMC cylinder was similar to PEC, and the cross-polarized component went toward zero in all regions. Therefore, the only effective parameters in anisotropic media were ε_3, μ_1, and μ_2 (see Table 1). In this figure, these parameters were used for both positive ($\varepsilon_3 = \mu_1 = \mu_2 = +1.5$) and negative ($\varepsilon_3 = \mu_1 = \mu_2 = -1.5$) values. Also ineffective parameters (ε_1, ε_2, and μ_3) were selected in both negative ($\varepsilon_1 = \varepsilon_2 = \mu_3 = -1.5$) and positive ($\varepsilon_1 = \varepsilon_2 = \mu_3 = 1.5$) values, respectively. It is obvious that the results had excellent agreement with [5].

Figure 4 presents the radiation patterns from PEMC cylinder with $M\eta_0 = \pm 1$ coated with anisotropic lossless media when $\varepsilon_1 = \varepsilon_2 = -\mu_1 = -\mu_2$, $\varepsilon_3 = -\mu_3$ (ε_3 and μ_2 have the same sign). Under these conditions for any radius of PEMC core ($0 < a \leq b$), there was no variation in the fields of both Regions I and II. In fact, these fields of Regions I and II did not depend on radius of PEMC core. Also, the fields in the anisotropic region (Region III) satisfied the PEMC medium conditions (see Appendix A), and this structure was equivalent to an uncoated PEMC cylinder with radius $\underline{b}$. Therefore, using the anisotropic medium, the radius of PEMC core was increased and the PEMC media realized. In this figure, outer radius of anisotropic media and location of line source were $b = 2.2\lambda_0$ and $\rho_0 = 2.3\lambda_0$, respectively.

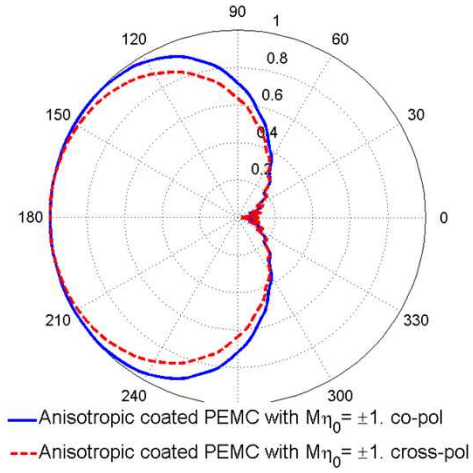

Figure 4. Far-field radiation patterns of electric line source outside a PEMC cylinder coated with anisotropic lossless layer with $b = 2.2\lambda_0$, $\rho_0 = 2.3\lambda_0$ and $\begin{cases} \varepsilon_1 = \varepsilon_2 \\ \mu_1 = \mu_2 \end{cases}$, $\begin{cases} \varepsilon_3 = -\mu_3 \\ \mu_2 = -\varepsilon_2 \end{cases}$, $\begin{cases} 0 < a \leq 2.2\lambda_0 \\ \varepsilon_i \neq 0 \text{ or } \pm\infty \end{cases}$.

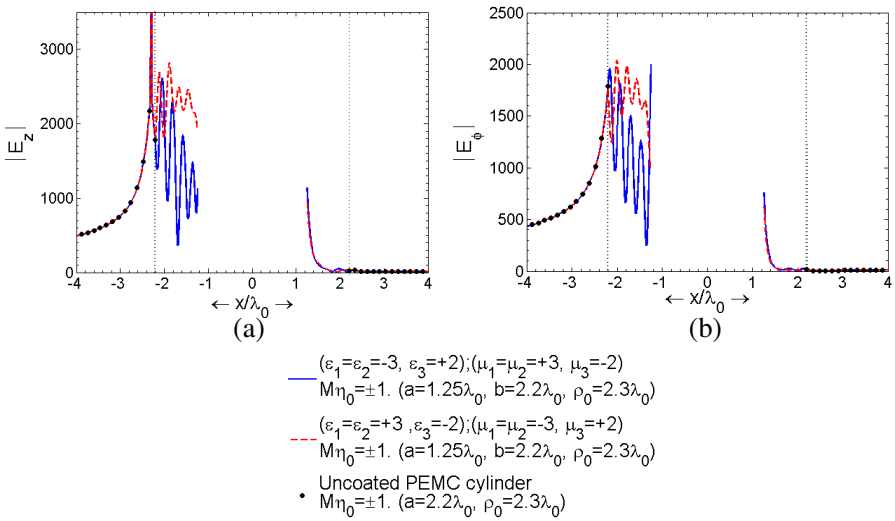

Figure 5. Magnitude of electric field inside and outside of anisotropic layer along the x-axes. (a) co- and (b) cross-pol components.

Figures 5(a) and (b) present the behavior of the co- and cross-polarized fields inside and outside the anisotropic region along the x-axis when $a = 1.25\lambda_0$, $b = 2.2\lambda_0$, and $\rho_0 = 2.3\lambda_0$. It is seen in Fig. 5(a) that the co-polarized component of field ($|E_z|$) exhibits a different behavior in anisotropic region ($a \leq \rho \leq b$) for two cases of 1) $\varepsilon_1 = \varepsilon_2 = -3$, $\varepsilon_3 = 2$, $\mu_1 = \mu_2 = 3$, $\mu_3 = -2$ and 2) $\varepsilon_1 = \varepsilon_2 = 3$, $\varepsilon_3 = -2$, $\mu_1 = \mu_2 = -3$, $\mu_3 = 2$. In contrast, in free space ($\rho \geq b$), the magnitudes of fields were independent from these parameters and completely matched with the uncoated PEMC cylinder with radius $2.2\lambda_0$. It is interesting to note that the behavior of cross-polarized component of field ($|E_\phi|$) was similar to the co-polarized case, as shown in Fig. 5(b).

4. CONCLUSIONS

In summary, the complete analytical solution was demonstrated for line source scattering from a PEMC circular cylinder coated with anisotropic media. Also, the parameters of the anisotropic media in TM_z and TE_z polarizations were selected as positive (μ_1, μ_2, $\varepsilon_3 > 0$) and negative (ε_1, ε_2, $\mu_3 < 0$) values, respectively, or vice versa. The results showed that the layer of anisotropic medium added to the small PEMC circular cylinder core could act as a PEMC boundary when the parameters of the structure were chosen in an appropriate manner. Although the small PEMC core was used for realizing the PEMC circular cylinder, the research might be useful for designing PECM cylinder with larger radius.

APPENDIX A. LINEAR MATRIX EQUATION AND REALIZATION OF PEMC CIRCULAR CYLINDER

The linear matrix equation obtained by boundary conditions at (17) to (22) are shown as follows:

$$\begin{bmatrix} 0 & 0 & M\eta_0 J_{\nu_e}(u_a) & M\eta_0 H^{(2)}_{\nu_e}(u_a) \\ 0 & 0 & -jY_e J'_{\nu_e}(u_a) & -jY_e H'^{(2)}_{\nu_e}(u_a) \\ -H^{(2)}_n(k_0 b) & 0 & J_{\nu_e}(u_b) & H^{(2)}_{\nu_e}(u_b) \\ -H'^{(2)}_n(k_0 b) & 0 & Y_e J'_{\nu_e}(u_b) & Y_e H'^{(2)}_{\nu_e}(u_b) \\ 0 & -H^{(2)}_n(k_0 b) & 0 & 0 \\ 0 & -H'^{(2)}_n(k_0 b) & 0 & 0 \end{bmatrix}$$

$$\begin{bmatrix} -jY_eJ_{\nu_m}(v_a) & -jY_eH^{(2)}_{\nu_m}(v_a) \\ M\eta_0Y_eZ_mJ'_{\nu_m}(v_a) & M\eta_0Y_eZ_mH'^{(2)}_{\nu_m}(v_a) \\ 0 & 0 \\ 0 & 0 \\ Y_eJ_{\nu_m}(v_b) & Y_eH^{(2)}_{\nu_m}(v_b) \\ Y_eZ_mJ'_{\nu_m}(v_b) & Y_eZ_mH'^{(2)}_{\nu_m}(v_b) \end{bmatrix} \begin{bmatrix} a_n \\ b_n \\ c_n \\ d_n \\ e_n \\ f_n \end{bmatrix} = \begin{bmatrix} 0 \\ 0 \\ J_n(k_0b) \\ J'_n(k_0b) \\ 0 \\ 0 \end{bmatrix} \quad \text{(A1)}$$

where $u_a = k_0a\sqrt{\mu_2\varepsilon_3}$, $u_b = k_0b\sqrt{\mu_2\varepsilon_3}$, $v_a = k_0a\sqrt{\mu_3\varepsilon_2}$, and $v_b = k_0b\sqrt{\mu_3\varepsilon_2}$. The above matrix equation can be shown as $AX = B$. In this case the unknown coefficients can be obtained by $X = A^{(-1)}B$ where $A^{(-1)}$ is the inverse of A. Therefore, the scattering coefficients in Region I and II are obtained by

$$a_n = A^{(-1)}(1,3)J_n(k_0b) + A^{(-1)}(1,4)\,J'_n(k_0b) \quad \text{(A2)}$$

$$b_n = A^{(-1)}(2,3)J_n(k_0b) + A^{(-1)}(2,4)\,J'_n(k_0b) \quad \text{(A3)}$$

Now for $M\eta_0 = \pm 1$, anisotropic lossless media are chosen with the following parameters

$$\begin{cases} \varepsilon_1 = \varepsilon_2 \\ \mu_1 = \mu_2 \end{cases}, \quad \begin{cases} \varepsilon_3 = -\mu_3 \\ \mu_2 = -\varepsilon_2 \end{cases} \text{ and } \quad \begin{cases} a > 0 \\ \varepsilon_i \neq 0 \ \& \ \pm\infty \ (i = 1,2,3) \end{cases} \quad \text{(A4)}$$

Likewise, the values of ε_3 and μ_2 should have the same sign (positive or negative), and the radius of PEMC core should not be close to zero (because singular points are created in the above matrix and because the cross-polarized component of fields vanishes in all regions). If the above appropriate conditions that result in $u = -v$, $\nu_e = \nu_m = n$, and $Y_e = Z_m$ are applied, the following relations are reached

$$A^{(-1)}(1,3) = -jA^{(-1)}(2,3) = \frac{-1}{2H^{(2)}_n(K_0b)} \quad \text{(A5)}$$

$$A^{(-1)}(1,4) = jA^{(-1)}(2,4) = \frac{-1}{2H'^{(2)}_n(K_0b)} \quad \text{(A6)}$$

Hence, using (A2), (A3), (A5), and (A6) the scattering coefficients can be written as

$$a_n = \left(\frac{-1}{2H^{(2)}_n(K_0b)}\right) J_n(k_0b) + \left(\frac{-1}{2H'^{(2)}_n(K_0b)}\right) J'_n(k_0b) \quad \text{(A7)}$$

$$b_n = \left(\frac{1}{j2H^{(2)}_n(K_0b)}\right) J_n(k_0b) + \left(\frac{-1}{j2H'^{(2)}_n(K_0b)}\right) J'_n(k_0b) \quad \text{(A8)}$$

It can be derived that these coefficients do not depend on anisotropic media and radius of PEMC core. Also, in anisotropic media, the relations between electric and magnetic fields just for $M\eta_0 = \pm 1$ are

$$\vec{H}^{III} + M\vec{E}^{III} = 0 \tag{A9}$$

$$\vec{D}^{III} + M\vec{B}^{III} = 0 \tag{A10}$$

In fact, applying these conditions (A4) leads to the anisotropic medium acted as PEMC media while a_n and b_n are the scattering coefficients from PEMC cylinder with the radius of $\underline{b}$. According to Equations (A9) and (A10), it can be clearly seen that the proposed anisotropic coat can be considered like a PEMC medium.

APPENDIX B. PLANE WAVE SCATTERING

When the line source is placed at far distance ($k_0\rho_0 \gg 1$, $\rho < \rho_0$) and the asymptotic form of Hankel function used, the following can be written

$$E_z^{inc} = E_0 \sum_{n=-\infty}^{+\infty} j^{+n} J_n(k_0\rho) e^{jn(\phi-\phi_0)} \tag{B1}$$

where $E_0 = \frac{-k_0^2 I_e}{4\omega\varepsilon_0}\sqrt{\frac{2}{\pi k_0\rho_0}}\, e^{-j(k_0\rho_0-\pi/4)}$. Equation (B1) represents the incident electric field of TM_z uniform plane wave of strength E_0 at angle ϕ_0 on a PEMC coated with anisotropic media. Therefore, the bistatic RCS can be written for TM_z polarization in the form

$$\sigma_{\text{co}}/\lambda_0 = \frac{2}{\pi}\left|\sum_{n=-\infty}^{+\infty} a_n e^{jn(\phi-\phi_0)}\right|^2; \quad \sigma_{\text{cross}}/\lambda_0 = \frac{2}{\pi}\left|\sum_{n=-\infty}^{+\infty} b_n e^{jn(\phi-\phi_0)}\right|^2 \tag{B2}$$

where a_n and b_n are the scattering coefficients of the co- and cross-polarized field components, respectively.

REFERENCES

1. Lindell, I. V. and A. H. Sihvola, "Perfect electromagnetic conductor," *Journal of Electromagnetic Waves and Applications*, Vol. 19, No. 7, 861–869, 2005.
2. Lindell, I. V. and A. H. Sihvola, "Losses in PEMC boundary," *IEEE Trans. on Antennas and Propag.*, Vol. 54, No. 9, 2553–2558, 2006.

3. Sihvola A. H. and I. V. Lindell, "Possible applications of perfect electromagnetic conductor (PEMC) media," *Proc. the 1st Eur. Conf. on Antennas and Propag., EuCAP*, 1–6, Nice, France, Nov. 2006.
4. Lindell, I. V. and A. H. Sihvola, "Realization of the PEMC boundary," *IEEE Trans. on Antennas and Propag.*, Vol. 53, 3012–3018, 2005.
5. Sun, J., W. Sun, T. Jiang, and Y. Feng, "Directive electromagnetic radiation of a line source scattered by a conducting cylinder coated with left-handed metamaterial," *Microw. Opt. Technol. Lett.*, Vol. 47, 274–279, 2005.
6. Ahmed, A. and Q. A. Naqvi, "Directive EM radiation of a line source in the presence of a coated PEMC circular cylinder," *Progress In Electromagnetic Research*, Vol. 92, 91–102, 2009.
7. Massoudi, H., N. J. Damaskos, and P. L. E. Uslenghi, "Scattering by a composite and anisotropic circular cylindrical structure: Exact solution," *Electromagnetics*, Vol. 8, 71–83, 1988.
8. Ahmed, A. and Q. A. Naqvi, "Electromagnetic scattering from a perfect electromagnetic conductor cylinder coated with a metamaterial having negative permittivity and/or permeability," *Opt. Communication*, 5664–5670, 2008.
9. Mehmood, M. Q. and M. J. Mughal, "Analysis of focal region fields of PEMC Gregorian system embedded in homogenous chiral medium," *Progress In Electromagnetics Research Letters*, Vol. 18, 155–163, 2010.
10. Ghaffar, A., N. Mehmood, M. Shoaib, M. Y. Naz, A. Illahi, and Q. A. Naqvi, "Scattering of a radially oriented hertz dipole field by a perfect electromagnetic conductor (PEMC) sphere," *Progress In Electromagnetics Research B*, Vol. 42, 163–180, 2012.
11. Shahvarpour, A., T. Kodera, A. Parsa, and C. Caloz, "Realization of the PEMC boundary," *IEEE Trans. on Antennas and Propag.*, Vol. 58, No. 11, 2781–2792, 2010.
12. Harrington, R. F, *Time-harmonic Electromagnetic Fields*, IEEE Press, Piscataway, NJ, 2001.